Carbohydrate Polymers 92 (2013) 11–18

Contents lists available at SciVerse ScienceDirect

Carbohydrate Polymers

journal homepage: www.elsevier.com/locate/carbpol

Surface acetylation of bamboo cellulose: Preparation and rheological properties

Jie Cai[a,b], Peng Fei[a,b], Zhouyi Xiong[a,b], Yongjun Shi[a,b], Kai Yan[a,b], Hanguo Xiong[a,b,*]

[a] College of Food Science and Technology, Huazhong Agricultural University, Wuhan 430070, China
[b] Research Institute of Comprehensive Utilization of Biomaterials, Huazhong Agricultural University, Wuhan 430070, China

ARTICLE INFO

Article history:
Received 13 August 2012
Received in revised form 29 August 2012
Accepted 24 September 2012
Available online 2 October 2012

Keywords:
Bamboo cellulose
B-CDA
Acetone/DMAc solvent system
Rheological properties
Spinnability

ABSTRACT

In this study, purified bamboo cellulose was used to synthesize cellulose diacetate (B-CDA). The synthesis was controlled by determination of the degree of substitution and insoluble residue content. The product then was characterized by FTIR. The rheological properties of B-CDA solutions in acetone/N,N-dimethylacetamide (DMAc) solvent system were systematically investigated on an advanced rheometer, including the dependence of apparent viscosity η_α, non-Newtonian index n, and structural viscosity index $\Delta\eta$ on the concentration and temperature of the solutions. B-CDA–acetone/DMAc solution is a shear-thinning fluid. With increasing solution concentration and decreasing temperature, $\Delta\eta$ increased, whereas n decreased, which indicates a deteriorating spinnability. Moreover, the values of the viscous flow activation energy E_η based on the Arrhenius equation increased when the shear rate γ was enhanced, which indicates that the η_α of the solution is more sensitive to temperature in the higher γ values. The results are favorable for predicting the B-CDA solution spinnability.

1. Introduction

With the rapid development of digitized video devices such as LCD monitors, the mechanical reinforcement of optically functional materials is of significant interest to various industries. Reinforcements that use environmentally friendly and renewable cellulose have been considered because natural cellulose can provide the desired mechanical reinforcement of optically functional materials. However, cellulose materials with components larger than the visible light wavelength seriously interfere with light transmission, which make them unsuitable for optical applications. Thus, nanocellulose prepared from natural raw materials exhibits remarkable characteristics, such as being infinitesimally tiny, with outstanding mechanical properties that can be perfectly applied to optically functional materials (Abe, Iwamoto, & Yano, 2007; Beecroft & Ober, 1997; Novak, 1993; Yano et al., 2005).

Compared with traditional methods such as physical and chemical techniques, the electrospinning technique is a more novel technique for fabricating nanomaterials, which has been widely used in the field of nanocellulose production due to the good controllability of the product size and morphology (Li & Xia, 2004; Sigmund et al., 2006; Thorvaldsson, Stenhamre, Gatenholm, & Walkenström, 2008). Cellulose, which is a linear polysaccharide consisting of β(1-4)-linked anhydroglucopyranose units, cannot dissolve in most common organic solvents because of extensive intra- and inter-molecular hydrogen bonding (Appaw, Gilbert, & Khan, 2007). As a result, cellulose is typically derivatized to facilitate dissolution in solvents for electrospinning. One of the most important cellulose derivatives is cellulose acetate (CA), which is obtained by native cellulose esterification in the presence of glacial acetic acid as a solvent, acetic anhydride as an acetylating agent, and sulfuric acid as a catalyst (Cerqueira, Filho, & Meireles, 2007; Edgar et al., 2001; Sassi & Chanzy, 1995; Steinmeier, 2004).

Bamboo, an abundant regenerative natural bioresource in Asia such as Chian, is a kind of fast-growing and early harvested vegetable. Bamboo cellulose has an important function in composites because of its small environmental load, low weight, high adaptability, and relatively high strength (Liu & Hu, 2008; Liu, Zhong, Chang, Li, & Wu, 2010; Nitayaphat, Jiratumnukul, Charuchinda, & Kittinaovarat, 2009; Wan et al., 2011). Thus, bamboo cellulose is an attractive candidate for strengthening natural cellulose. There is little report about bamboo cellulose used in CA preparation.

Bamboo cellulose was purified to achieve a α-cellulose content and brightness of 96.37% and 90%, respectively, which suited the preparation requirements of commercially available CAs that were used in this study. Subsequently, bamboo cellulose triacetate (B-CTA) was first synthesized from purified bamboo cellulose in a general acetylation medium containing glacial acetic acid, acetic anhydride, and sulfuric acid. B-CTA was then hydrolyzed to produce bamboo cellulose diacetate (B-CDA), which facilitated the dissolution in an acetone/N,N-dimethylacetamide (DMAc) (2:1, by weight) solvent system. The rheological properties of

* Corresponding author at: College of Food Science and Technology, Huazhong Agricultural University, Wuhan 430070, China. Tel.: +86 27 87288377; fax: +86 27 87286608.
E-mail address: xionghanguo@163.com (H. Xiong).

0144-8617/$ – see front matter © 2012 Elsevier Ltd. All rights reserved.
http://dx.doi.org/10.1016/j.carbpol.2012.09.059

B-CDA–acetone/DMAc solutions were systematically investigated using an advanced rheometer and are favorable for predicting the solution spinnability, which is particularly significant before using this solution in the spinning process.

2. Experimental method

2.1. Materials

The commercial bleach bamboo cellulose used in these experiments was supplied by Guangxi Jia Yu Paper Pulp Co., Ltd. with a α-cellulose content and brightness of 76.73% and 80%, respectively. Methylene dichloride was produced from Shanghai Gaoyun Chemical Co., Ltd. Glacial acetic acid, acetic anhydride, sodium hydroxide, sulfuric acid, hydrochloric acid, methanol, magnesium acetate, ethyl alcohol acetone and N,N-dimethylacetamide (DMAc) were purchased from Sinopharm Chemical Reagent Co., Ltd. All chemicals were of analytical reagent grade and used without further purification.

2.2. Bamboo cellulose purification

Bamboo cellulose purification was performed as follows: a mixture of oven-dried cellulose and 10 wt% sodium hydroxide solution (solid-to-liquid ratio – 1:50, w/w) was left in a polyethylene (PE) plastic bag and kneaded every 15–20 min. After 1 h, the mixture was filtered and washed with distilled water to attain a neutral pH. The pre-treated sample was dried in a vacuum oven (pressure of 30 mm) at 105 °C for 5 h.

2.3. Preparation of bamboo cellulose diacetate (B-CDA)

Cellulose acetylation was carried out using a previously described process as follows (He, Ming, Cui, & Wang, 2009; Rodrigues, Silva, Meireles, Assuncao, & Otaguro, 2005): the well-purified and dried cellulose (5 g), which was introduced in a three-necked, round-bottom flask equipped with an overhead stirrer, was activated by impregnation in glacial acetic acid (9 mL of acetic acid for each gram of cellulose). This treatment comparison was conducted by another impregnation in 18 wt% solution of sodium hydroxide. The activated cellulose was then acetylated with a mixture of 25 mL of acetic anhydride containing sulfuric acid as a catalyst at a fixed temperature of 50 °C for 2.5 h. The catalyst content was 4.5% (v/m) of purified cellulose.

After stopping the reaction, the bamboo cellulose triacetate (B-CTA) solution system was then heated to 60 °C and added with the hydrolysis mixture (acid catalyst and acetic acid aqueous solution) while stirring for hydrolysis to begin. In successive experiments, the mixture was mechanically stirred for 3 h to obtain the desired degree of substitution (DS). Subsequently, an excessive amount of 21–24 wt% aqueous magnesium acetate solution was added to neutralize the sulfuric acid. After completing the whole reaction, distilled water was slowly poured into the reaction medium with constant stirring until no more precipitate was formed. The produced bamboo cellulose diacetate (B-CDA) was separated by vacuum filtration and washed with distilled water to achieve a neutral pH. Finally, the sample was dried in a vacuum oven (pressure of 30 mm) for 6 h at 60 °C.

2.4. Chemical analysis

2.4.1. Determination of the degree of substitution (DS)

The chemical degree of substitution (DS) is the average value of $-COCH_3$ groups that replace hydroxyls in every glucose cycle. The DS of the acetylated samples were determined through a saponification reaction (ASTM D 871-96), as follows.

Dry about 1 g of the sample was accurately weighed then transferred to a 250 mL conical flask. Approximately 40 mL of ethyl alcohol (75 vol%) was added to the flask, which was then warmed to 60 °C for 30 min. Subsequently, 50 mL of 0.5 N NaOH was added to the system, which was again heated at 60 °C and left to stand for 15 min. The same procedure also included blank determination and back titration with each set of samples for a control system. The flasks were tightly stoppered and allowed to stand at 25 °C for about 72 h. The excess alkali in the sample was titrated with 0.5 N HCl using phenolphthalein as the indicator. An excess of about 1 mL of HCl was added, and NaOH was allowed to diffuse from the sample overnight.

The disappearance of the pink color in the solution indicated the complete neutralization of NaOH. The slight excess of HCl was then back titrated with NaOH (0.5 N) to a phenolphthalein end point (i.e., until the faint pink color was observed in the solution after vigorously shaking the flask). The percentage of combined acetyl was calculated from Eq. (1):

$$\text{Acetyl\%} = \frac{[(V_4 - V_3)N_{\text{NaOH}} + (V_1 - V_2)N_{\text{HCl}}] \times 4.305}{W} \quad (1)$$

To determine DS of the sample, Eq. (2) was defined as:

$$\text{DS} = \frac{3.86 \times \text{Acetyl}(\%)}{102.40 - \text{Acetyl}(\%)} \quad (2)$$

where V_1 = NaOH volume required for titration of the sample; V_2 = NaOH volume required for titration of the blank; V_3 = HCl volume required for titration of the sample; V_4 = HCl volume required for titration of the blank; N_{NaOH} = NaOH concentration; N_{HCl} = HCl concentration; W = weight of the sample.

2.4.2. Determination of the insoluble residue content (IRC)

Approximately 2.00 g of the sample was introduced in a l00 mL round-bottom flask fitted with an overhead stirrer. About 40 mL of methylene dichloride/methanol (9:1, v/v) mixture was then added to the mixture. After adding the solution, stirring continued for 2 h at room temperature. The reaction solution was centrifuged at 3000 rpm for 30 min to separate the soluble and insoluble portions. The supernatant was then pipetted out, and the residue was washed three times with mixed reagent. Finally, the soluble portions and the insoluble residue were washed with ethyl alcohol (95 vol%) for stabilization and dried in a vacuum until a constant weight was achieved.

Eq. (3) was used in order to determine the insoluble residue content (IRC).

$$\text{IRC} \ (\%) = \frac{M}{m_{\text{total}}} \times 100 \quad (3)$$

where M is the weight of the insoluble residue and m_{total} is the weight of the sample.

2.5. Preparation of B-CDA–DMK/DMAc solutions

The various contents of the B-CDA sample were dissolved in acetone/DMAc (2:1, by weight) system with mechanical stirring for 1.5–2 h at room temperature. The homogenous and transparent B-CDA–acetone/DMAc solutions were obtained with mass concentrations of 17, 19, 21, 22, 23, and 24 wt%.

2.6. Rheological behavior measurements

Rheological measurements were performed on an AR 2000 rotational rheometer with a parallel plate geometry, a diameter of 40 mm, and flat gap of 1 mm. The parallel plate periphery was covered with a thin layer of low-weight silicon oil to minimize evaporation losses during the experiments. The shear stress

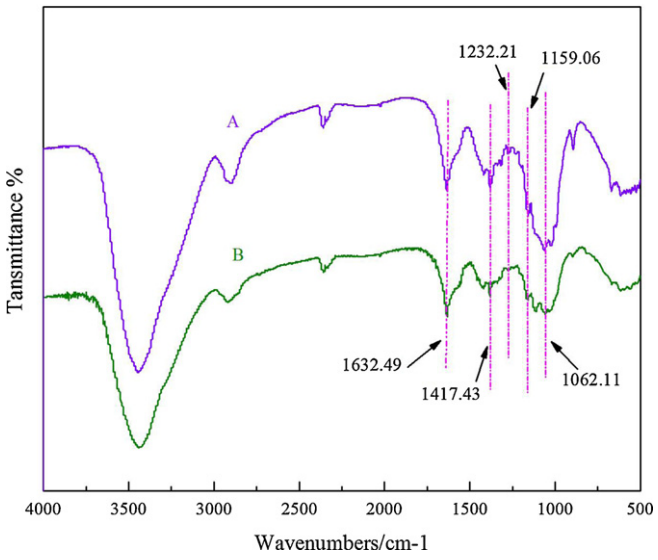

Fig. 1. FTIR spectra of (*A*) pristine cellulose and (*B*) purified cellulose.

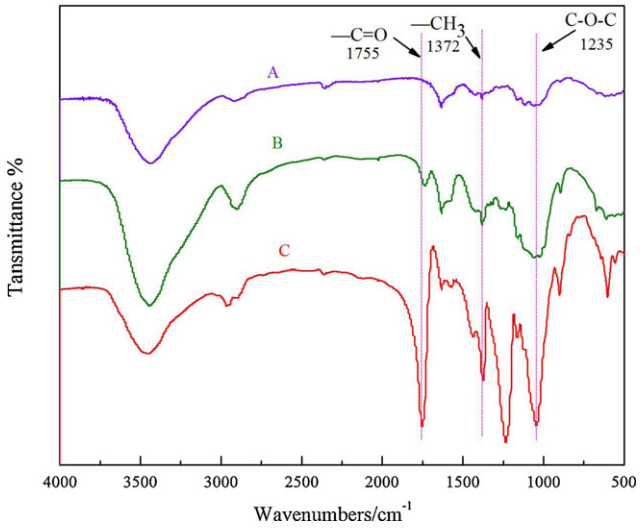

Fig. 2. FTIR spectra of unmodified cellulose (*A*) and celluloses activated with acetic acid glacial (*B*) and with 18% solution of sodium hydroxide (*C*).

(τ)–shear rate (γ) and apparent viscosity (η_α)–shear rate (γ) dependencies of the different B-CDA concentration solutions were measured at various shear rates ranging from 0.001 s^{-1} to 400 s^{-1} over 20–70 °C. All measurements were performed in triplicates.

2.7. Fourier transform infrared (FTIR) spectroscopy

FTIR spectra of the sample were recorded with a Nexus-470 Fourier Transform Infrared Spectrophotometer. Thirty-two scans were accumulated for each spectrum at a resolution of 4 cm^{-1} in the region from 4000 to 400 cm^{-1}, using KBr pellets (1 mg power of samples/100 mg KBr).

3. Results and discussion

3.1. Bamboo cellulose purification analysis

After purification, the bamboo cellulose with 96.37% α-cellulose content and 90% brightness becomes suitable for the production requirement of commercially available CAs. Apart from chemical determination, Fourier transform infrared spectroscopy (FTIR) was also used to study cellulose purification. Fig. 1 depicts the decreasing absorption intensity of the bands mainly located at 1632.49 cm^{-1}, which is generally assigned to the stretching of the lignin carbonyl groups. Other important aspects observed in the IR spectrum are the reduced intensities of the bands at 1417.43 cm^{-1} (aromatic ring vibrations of the phenylpropane skeleton), 1232.21 cm^{-1} (aryl–alkyl ether linkage), and 1159.02 cm^{-1} (lignin-alkyl ether base antisymmetric bridge stretching). This characteristic indicates that lignin, hemicelluloses, and other impurities were more effectively removed from this cellulose. On the other hand, the chromophore groups and the auxochrome groups presented lower intensity bands after purification (1062.11 cm^{-1} assigned to C=O stretching as an example), which corresponds to a higher whiteness of pre-treated cellulose.

3.2. Characterization of the produced cellulose acetates

Bamboo cellulose was activated by two different methods, namely, 18 wt% solution of sodium hydroxide and acetic acid glacial activation. The activation conditions are shown in Table 1. The FTIR analysis of the samples at the same acetylation conditions and in different activation conditions is illustrated in Fig. 2. Curve *A* represents the IR spectrum of unmodified cellulose. Curves *B* and *C* correspond to the acetylated celluloses prepared in different activation conditions 1# and 2# as indicated in Table 1, respectively. Curves *B* and *C* have several differences compared with curve *A*. The IR spectra of the acetylated samples are at the expected acetyl group vibrations of 1755 cm^{-1} (—C=O) and 1235 cm^{-1} (C—O—C). Moreover, the frequency band at 1375 cm^{-1} shows peaks of great intensity, which are attributed to —C—H bending vibration and —C—CH_3 stretching vibration in the spectra of native and acetylated cellulose, respectively. Fig. 2 also shows the comparison between the effect of activation conditions 1# and 2#. From Fig. 2, activation condition 2# is better than activation condition 1# in promoting bamboo cellulose acetylation because the area of the —C=O peak in curve *C* is larger than that of curve *B*. During the activation process of method 1#, the activated bamboo celluloses were washed with distilled water to obtain a neutral pH in case sodium hydroxide reacts with acetic anhydride. Water permeation in bamboo cellulose causes acetic anhydride hydrolysis, which inhibits the acetylation reaction. However, in the activation process of method 2#, bamboo celluloses were activated with glacial acetic acid, which can easily enter the crystalline region and inhibit acetic anhydride hydrolysis. The results in Table 1 also show that method 2# is the better activation method for its shorter activation time, higher acetylation degree, and lower insoluble residue content. The results agree with those inferred from Fig. 2.

Fig. 3 shows the (i) FTIR spectra of the reaction mixtures in the esterification process and (ii) FTIR spectra of native cellulose, B-CTA and B-CDA.

As shown in Fig. 3(i), curves A_i, B_i, and C_i represent the reaction mixtures removed from the acetylation medium at 15, 30, and 90 min, respectively. The mixtures can be monitored by the absorption band at 1827.76 cm^{-1} assigned to C(O stretching (acetic anhydride), at 1755.81 cm^{-1} assigned to C=O stretching (acylation product), and at 1722.14 cm^{-1} assigned to C=O stretching (glacial acetic acid). The absorption intensity of the bands located at 1755.81 and 1722.14 cm^{-1} increased, but the band intensity at 18,277.76 cm^{-1} decreased with increasing reaction time (Fig. 3). In the acylation process, the synthetic product is continuously dissolved in the reaction system, which exposes new hydroxyl groups on the cellulose surface. These new hydroxyl groups take part in the reaction again, which leads to declined acetic anhydride content but increased product content. The acetylation reaction of bamboo cellulose is continued until the system becomes homogeneous.

Table 1
The different activation conditions for bamboo cellulose, and DS and IRC of the products.

Method	Activation agent	Activation time (h)	Activation temperature (°C)	Acetylation time (h)	DS	IRC (%, w/w)
1#	Sodium hydroxide	2	20	2	2.22	26.69
2#	Acetic acid glacial	3	30	2	0.18	55.74

The DS values of cellulose acetate have a great influence on solubility. The CA samples with DS values above 2.8 (CTA) are only soluble in chloroform, but the CA samples with DS values from 2.2 to 2.7 (CDA) are soluble in acetone (Cao et al., 2007). In order to obtain the acetone/DMAc-soluble B-CDA, the hydrolysis of prepared B-CTA was carried out to form products with the desired DS. As shown in Fig. 3(ii), curves A_{ii}, B_{ii}, and C_{ii} correspond to native cellulose, B-CDA, and B-CTA with different DS of 0, 2.48, and 2.84, respectively. The B-CTA and B-CDA samples show similar spectral features, which present an appearance of a —CH_3 band at 1375 cm^{-1} as well as a strong intensity band at 1752 cm^{-1} for the C=O group from acetate. Comparing with native cellulose, these added groups characterize the material as an acetylated cellulose derivative, namely, CA. Additionally, a broad band located at about 3400 cm^{-1} exists, which corresponds to the —OH group stretching in the cellulose acetate spectrum. The ratio between these two bands (1752 cm^{-1}/3400 cm^{-1}) is used as a measure of the DS level. A high ratio signifies a sample with a high DS because the cellulose hydroxyl group is replaced by an acetate group during the acetylation reaction (Hurtubise, 1962). An increase in the adsorption at 1752 cm^{-1} in the B-CTA sample than in the B-CDA sample was observed (Fig. 3(ii)), which corroborates with the chemical DS.

3.3. Characterization of the flow curves for B-CDA–DMK/DMAc solutions

As is well known, the fluid flow behavior is an important index of the quality and volatility of spinning fluid, and directly affects spinnability. The shear stress (τ) and apparent viscosity (η_α) were determined as a function of the shear rate (γ) using an advanced rheometer to describe the general flow behavior of a fluid. For the presentation of the data either the τ or η_α is plotted against the γ. Thus, the obtained graph is defined as a rheogram (or flow curve). The resulting flow curve shows the relationship between these two fluid properties, namely, Newtonian fluid and non-Newtonian fluid flow characteristics.

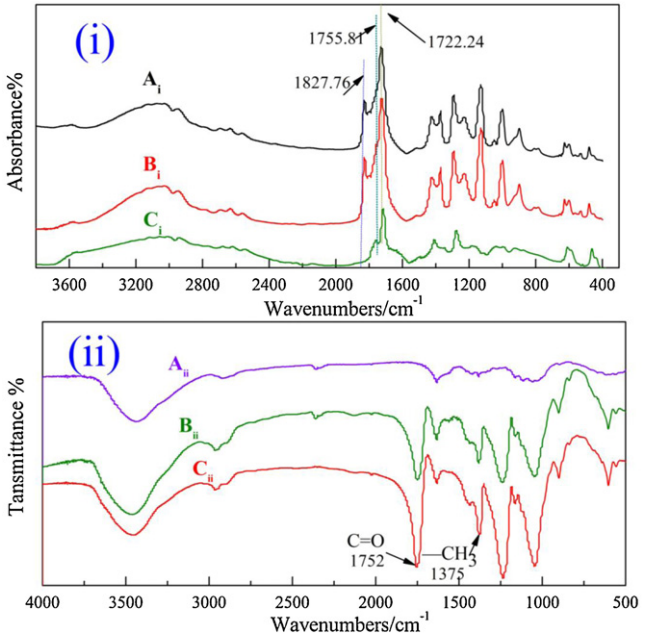

Fig. 3. (i) FTIR spectra of reaction mixtures of esterification process at (A_i) 15, (B_i) 30 and (C_i) 90 min. (ii) FTIR spectra of (A_{ii}) native cellulose, (B_{ii}) B-CDA and (C_{ii}) B-CTA with different DS of 0, 2.48, and 2.84.

For a Newtonian fluid, in which the η_α is independent of the γ, can be evaluated by using the Newtonian Model (Eq. (4)) (Rao, 2007, chap. 2):

$$\eta_\alpha = \frac{\tau}{\gamma} \tag{4}$$

The shear stress (τ) and the shear rate (γ) are proportional to each other, and a parameter (η_α), the apparent viscosity, characterizes the value. The flow curve of a Newtonian fluid is linear, and the slope of the straight line corresponds to the η_α.

Non-Newtonian fluids, however, behave differently, and their flow curves are generally curved lines with various shapes which are usually presented in exponential function (Eq. (5)) (Rao, 2007, chap. 2).

$$\eta_\alpha = K\gamma^{n-1} \tag{5}$$

For the exceptional case of a Newtonian fluid (flow index $n = 1$), the consistency index K is identically equal to the viscosity of the fluid, η_α. When the value of $n > 1$ the fluid is shear-thickening and when the value of $n < 1$ the fluid is shear-thinning in nature.

3.3.1. Different concentrations of the flow curve

The τ and η_α dependence of γ was investigated in the B-CDA concentration range of 17–24 wt% to determine the B-CDA–acetone/DMAc solution flow regimes and the influence of B-CDA concentration on solution shear flow. The flow curve for the investigated solutions was observed in the 20–70 °C interval corresponding to Fig. 4a–f. As shown in Fig. 4g, when γ, decreased, η_α gradually decreased for all concentration conditions in this experimental temperature range. This shear-thinning behavior indicates that B-CDA–acetone/DMAc solutions are typical non-Newtonian fluids (pseudoplastic fluids). At the same temperature, the B-CDA system with a higher solution concentration showed more remarkable pseudoplastic characteristics. When the B-CDA solution concentration was below 17 wt%, τ and η_α were affected less by γ, which exhibits approximate Newtonian fluid flow characteristics. In a B-CDA/acetone/DMAc system, a strong hydrogen bond exists among hydroxyl groups on cellulose macromolecules, carbonyl unit in acetone, and acetyl groups on DMAc. Thus, the B-CDA system, can form macromolecular chain entanglement and maintain an irregular internal order at rest, which makes the relative motion of cellulose macromolecules difficult (higher value of viscosity). The entanglement crosslinks in the B-CDA solution is rebuilt and consistently destroyed, while a dynamic equilibrium is achieved in a specific condition. Each of the macromolecular chain aggregates only function as a temporary crosslink when γ increases, intermolecular resistance, intermolecular action, and the crosslinks are destroyed, which results in shear-thinning. Meanwhile, the macromolecular chain segments among entanglement crosslinks could not relax and were probably oriented parallel to the flow field. Thus, the ability to transport energy among solvated layers decreases. The driving force among flow fields decreases, which could also allow the macromolecular chains to slip past one other easily and decreases the η_α. Another

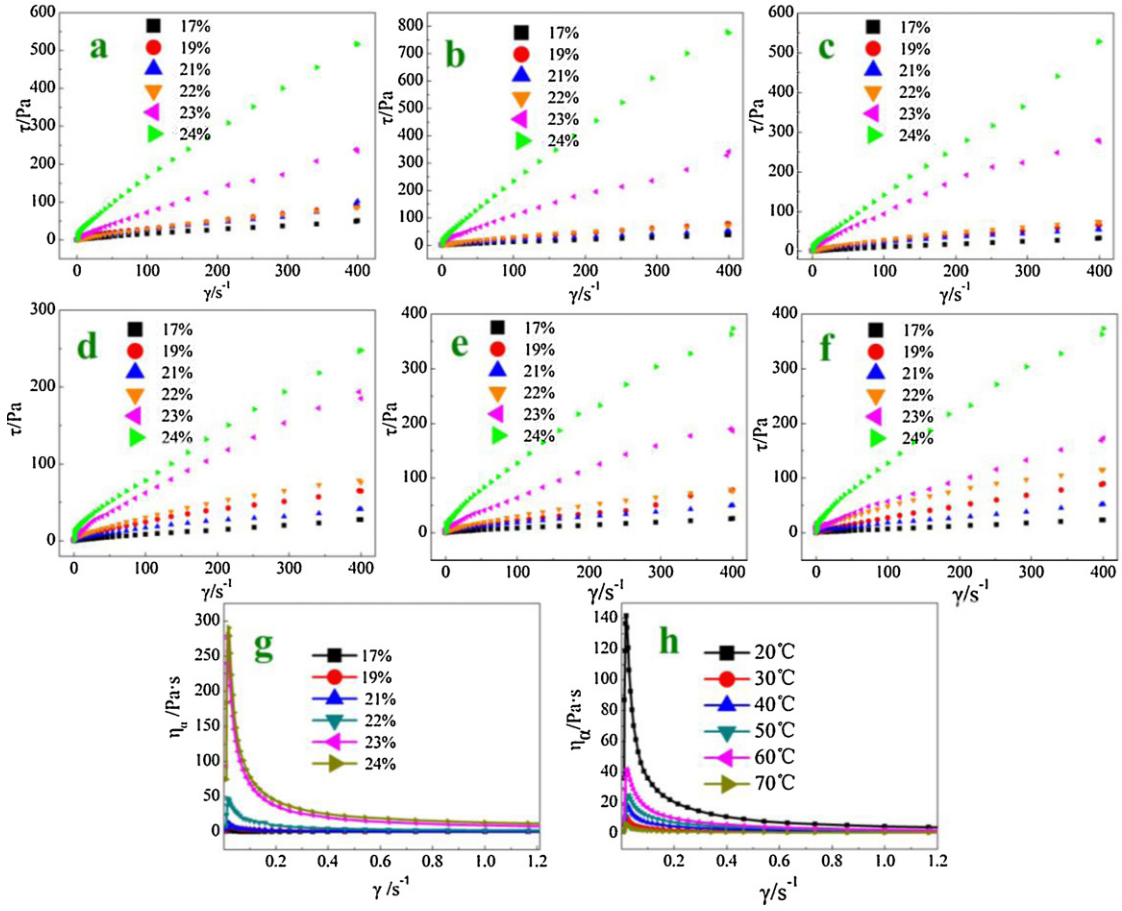

Fig. 4. Flow curves $\tau(\gamma)$ of B-CDA–acetone/DMAc solutions with different concentrations at (a) 20, (b) 30, (c) 40, (d) 50, (c) 60 and (d) 70 °C, and flow curves $\eta_\alpha(\gamma)$ for B-CDA solutions with different concentrations at 30 °C (g) and with different temperatures in the 21 wt% B-CDA concentration (f).

explanation for this phenomenon is the progressive shearing of flow layers with increasing γ, which decreases the interaction among cellulose macromolecules and leads to a consequent drop in shear viscosity. When the added B-CDA samples are increased, the hydrogen bond among B-CDA–acetone/DMAc solutions becomes stronger, which corresponds to an increase in τ at the same temperature.

3.3.2. Different temperature of the flow curve

The viscosity profiles for a 21 wt% B-CDA solution at different temperatures were plotted to investigate the effect of temperature on the decrease in viscosity (Fig. 4h). As shown in Fig. 4h, the true flow curves also showed a clear shear-thinning phenomenon, which indicates that the B-CDA–acetone/DMAc solutions are typically pseudoplastic fluids. In the range of 20–70 °C, the solutions progressed from strongly pseudoplastic to mildly pseudoplastic viscous flow behavior. At low temperatures (up to 20 °C), pseudoplastic characteristics are highly remarkable. However, a further increase to 70 °C results in η_α being less affected by γ, which is close to the Newtonian fluids. The η_α value of the B-CDA solution is very sensitive to temperature. As the measuring temperature increases, the macromolecular chain can disentangle and stretch, which easily allows the relative motion of cellulose macromolecules. This result corresponds to the decreased η_α of the solutions. At low temperatures, the hydrogen bond forms and the intermolecular entanglement crosslink increases, which translate to increased B-CDA solution viscosity.

3.4. Non-Newtonian index n of B-CDA–acetone/DMAc solutions

It is a common practice in the research to apply the Power Law Model (Ostwald-de-Waele model) to describe the non-Newtonian flow characteristics of most polymer solutions in theoretical analysis as well as in practical applications (Marcotte, Hoshahili, & Ramaswamy, 2001). Therefore, the flow properties of B-CDA–DMK/DMAc solutions were evaluated by using the Power Law equation (Eq. (6)):

$$\tau = K\gamma^n \tag{6}$$

where the parameter K, the consistency coefficient, is sometimes referred to as a viscosity related constant, and the exponent n, the power law index, is dimensionless value that reflects the closeness to Newtonian fluid flow.

To deal conveniently with the operation, Eq. (6) can be rewritten in a logarithmic form as:

$$lg\ \tau = lg\,K + n\,lg\,\gamma \tag{7}$$

The plots of $\ln\tau$ versus $\ln\gamma$ for a B-CDA concentration of 17–24 wt% (according to Eq. (7)) are shown in the 20–70 °C interval corresponding to Fig. 5a–f. Accordingly, the non-Newtonian index n is obtained from the slope. Fig. 5g displays the flow index n in the form of $n = f(C)$, where n is smaller than 1. The flow index sharply decreased until 21 wt%, and thereafter slowly decreased with increasing B-CDA concentrations at 30 °C. The entanglement crosslinks in the investigated solutions initially formed less frequently at lower temperatures. The then intermolecular resistance

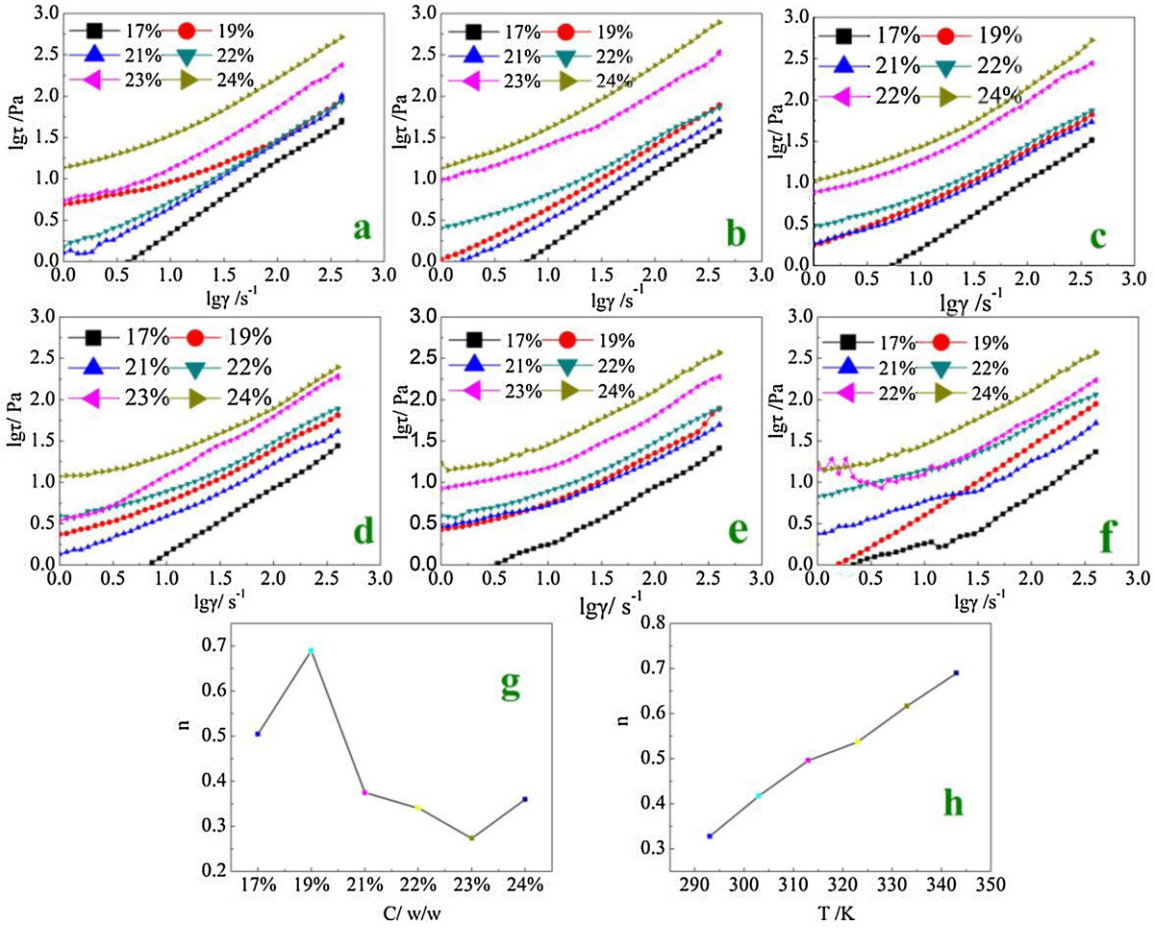

Fig. 5. ln τ/ln γ dependence on B-CDA concentration at (a) 20, (b) 30, (c) 40, (d) 50, (e) 60 and (f) 70 °C. Dependence of n on B-CDA concentration at 30 °C (g) and on solution temperature of 21 wt% B-CDA concentration (h).

increases, whereas cellulose macromolecular chain free activities decrease with increasing B-CDA concentrations in solutions. This result leads to the increased extent of fleeing from Newtonian fluid. The curve for n in the form of $n = f(T)$ is given in Fig. 5h, which corresponds to 21 wt% B-CDA solution. As shown in Fig. 5h, increasing the temperature results in the gradual shift of the exponent n to a higher value within the range 0–1. This gradual shift is due to the relative motion resistance of cellulose macromolecules, the entanglement crosslinks, and the extent of deviation from the Newtonian fluid, which decreases with the measured temperature. Therefore, the dependence of n on concentration and temperature of the solutions directly reflects the spinnability of the B-CDA solutions.

3.5. Structural viscosity index $\Delta\eta$ of B-CDA–acetone/DMAc solutions

The structural viscosity index ($\Delta\eta$) is another significant parameter that measures the spinnability of polymer melts and the quality of cellulose derivative. $\Delta\eta$, defined as follows, demonstrates the extent of structuralization of the spinning solution (Xu, Li, Yu, & Cao, 2008).

$$\Delta\eta = -\left(\frac{d\ \lg\eta_\alpha}{d\gamma^{1/2}}\right) \times 10^2 \quad (8)$$

where $\Delta\eta$ is structural viscosity index. η_α and γ denote the apparent viscosity and the shear rate, respectively.

Aforementioned, intermolecular resistance and macromolecular entanglement could result in numerous instant physical crosslinking sites in the B-CDA solution. These entanglement crosslinking sites counteract the orientation of cellulose macromolecules during the spinning process, thereby affecting B-CDA quality. When $\Delta\eta$ increases, the spinnability of the B-CDA solution becomes worse, which degrades the mechanical properties of cellulose. Reducing $\Delta\eta$ can weaken the structuralizing tendency of the spinning flow and, therefore, improve spinnability.

Fig. 6a–f depicts the $\lg\eta$–$\gamma^{1/2}$ curves for B-CDA concentrations between 17 wt% and 24 wt% at different temperatures. The B-CDA–acetone/DMAc solutions belong to the shear shinning fluid. The B-CDA–acetone/DMAc solutions belong to the shear shinning fluid. Tested the B-CDA–acetone/DMAc solutions belong to the shear shinning fluid, so, their $\Delta\eta$ is all greater than 0. According to Fig. 6, η_α decreases with increasing γ, which indicates that $\Delta\eta$ is always larger than 0. This result agrees with previous conclusions. This phenomenon also occurs because shear stress partly destroys the intermolecular entanglement crosslinks, orients the chain segments, and dissolves cellulose. The structural viscosity indices of B-CDA solutions with different concentrations at 30 °C are illustrated in Fig. 6g. Along with increasing B-CDA concentrations, $\Delta\eta$ also rose sharply. The sample concentration increments possibly led to an increased collision chance among the cellulose molecules, which promoted the formation of macromolecular chain entanglements. Thus, the degree of B-CDA system structuralization sharply increased, which indicated that solution spinnability worsened and cellulose formation became extremely difficult. In addition, the $\Delta\eta$

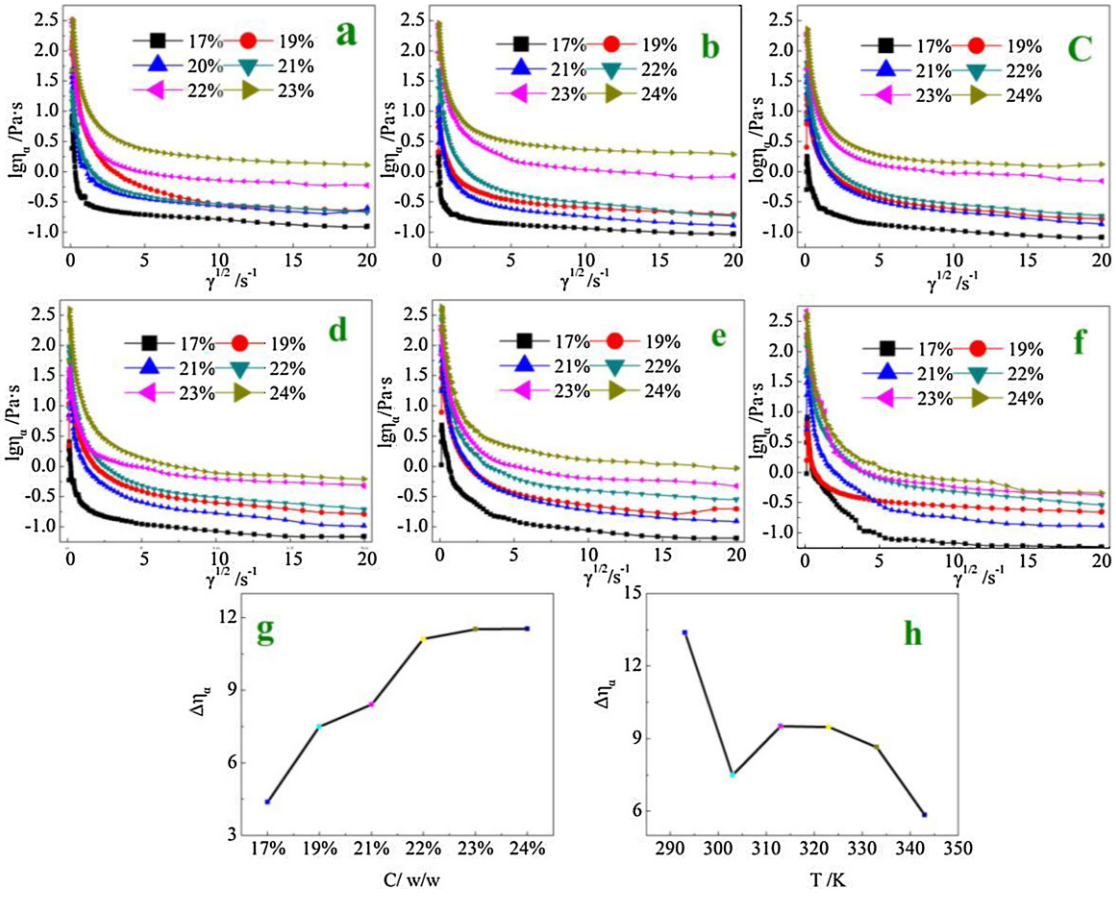

Fig. 6. lg η_α–$\gamma^{1/2}$ curves for B-CDA concentration at (a) 20, (b) 30, (c) 40, (d) 50, (e) 60 and (f) 70 °C. Dependence of $\Delta\eta$ on concentration at 30 °C (g) and on solution temperature of 21 wt% B-CDA concentration (h).

values of the B-CDA solutions are also affected by temperature. Fig. 6h indicates the dependence of $\Delta\eta$ on measured temperatures in the 21 wt% B-CDA concentration, from which $\Delta\eta$ was found to decrease slightly with increasing temperature. An elevated temperature possibly led to the increased distance between the cellulose molecules, which reduced the formation of cellulose chain aggregates. Accordingly, the extent of B-CDA system structuralization occurred at a slightly lower level, which is favorable for improving the B-CDA solution spinnability. However, a higher temperature would result in a higher collision chance among the cellulose molecules and cause spinning solution instability in the spinning process. Therefore, controlling the B-CDA concentration and solution temperature during the spinning process is extremely important.

3.6. Viscose flow activation energy E_η of B-CDA–acetone/DMAc solutions

A range of temperatures is employed during the spinning of cellulose solutions. Thus, the influence of temperature on viscosity needs to be documented. A common way to analyze the effect of temperature on the viscosity of the B-CDA solutions at a specified γ is through the use of the Arrhenius equation:

$$\eta_\alpha = A \ \exp\left(\frac{\Delta E_\eta}{RT}\right) \tag{9}$$

Rearranging Eq. (9) as follows is most convenient:

$$\ln \ \eta_\alpha = \ln A + \frac{E_\eta}{RT} \tag{10}$$

where E_η is the viscose flow activation energy of solution. T and η_α are the absolute temperature and apparent viscosity, respectively. R is the universal gas constant with a recommended value of $R = 8.314$ J/K mol and constant A is a frequency factor.

The viscous flow activation energy, E_η, is a useful measurement of the dependence of solution viscosity on temperature and also indicates the minimum energy needed by the reactants to undergo

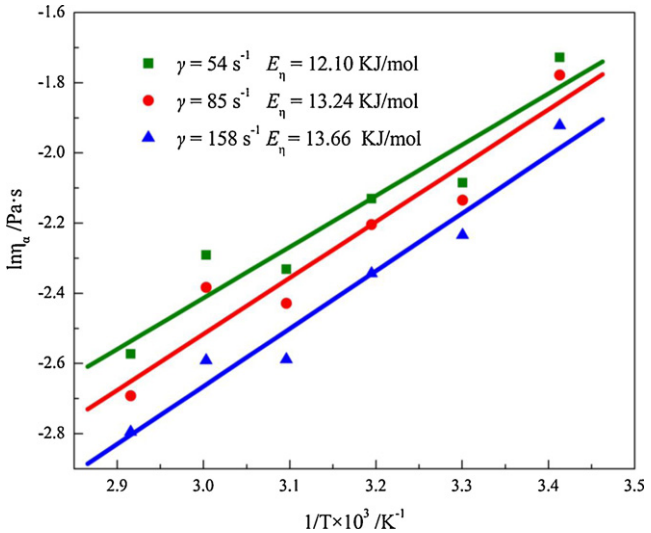

Fig. 7. Dependence of η_α on temperature of B-CDA–acetone/DMAc solutions with different γ.

reaction. A high E_η value means that the effect of temperature on solution viscosity is also high. Changing fluid ability is possible via temperature variation. The rising temperature promotes the relative motion of cellulose macromolecules and the expansion of solution space. Thus, the space between cellulose molecules becomes exaggerated and the fluid ability of solution improves, which accounts for the decrease of η_α.

According to Eq. (10), the Arrhenius plots of $\ln \eta_\alpha$ versus inverse temperature, $1/T$, for the 21 wt% B-CDA solutions as a measurement example at several shear rates are shown in Fig. 7. Approximating each set of testing data with a linear dependence is possible, as shown by the solid line for each γ. E_η is usually determined from the slope of the Arrhenius plots, which are summarized in Fig. 7. The E_η values of the B-CDA solution at a fixed γ slightly increased with increasing experimental temperature, which is related to the change in fluid ability of a solution. Moreover, E_η slightly increases as γ increases, which indicates that η_α of the B-CDA solution is more sensitive to temperature in higher γ values.

4. Conclusions

Bamboo cellulose was purified using a sodium hydroxide solution to achieve a 96.37% α-cellulose content and a 90% brightness, which are considered suitable for the preparation requirements of commercially available CAs. Purified bamboo cellulose was used for the synthesis of B-CDA via activation reaction, acetylation reaction, and hydrolysis, which were controlled by determining DS and IRC. The product was then investigated by FTIR. The prepared B-CDA sample was directly dissolved in an acetone/DMAc solvent system, and the rheological properties were systematically investigated by an advanced rheometer.

In this study, the activation method using glacial acetic acid is better than using sodium hydroxide solution because the former has a shorter activation time, higher DS, and lower IRC, which correspond to the changes in characteristic absorbances in FTIR spectra. Using the IR spectra to trace the esterification process, the acetylation reaction of bamboo cellulose continues until the system becomes homogeneous. From the IR analysis results, the newly added acyl groups characterize the reaction product as an acetylated cellulose derivative, namely, CA, as opposed to native cellulose. Moreover, the expected adsorption at 1752 cm^{-1} (—C=O) increased in the B-CDA (DS = 2.48) sample compared with the B-CTA sample (DS = 2.84), which is in accordance with the chemical DS. According to the flow curves, the B-CDA/acetone/DMAc solution is a typical shear-thinning fluid. The changes in the B-CDA concentration and the measured temperature have different influences on the non-Newtonian index n. In the studied B-CDA concentration range, the n values are smaller than 1.0 and continually decrease with increasing B-CDA concentration. In the studied temperature range, the exponent n gradually increases as the temperature increases. In addition, with increasing B-CDA concentration, $\Delta\eta$ sharply increased, yet slightly decreased with increasing temperature. Therefore, controlling the B-CDA concentration and solution temperature during the spinning process is extremely important. E_η slightly increases as γ increases, which indicates that η_α of the B-CDA solution is more sensitive to temperature in higher γ values. The results are favorable for predicting the spinnability of the B-CDA/acetone/DMAc solution, being particularly significant before using this solution in the spinning process.

Acknowledgments

The authors gratefully acknowledge the financial assistance supported by Huazhong Agricultural University Outstanding Graduate Student Innovation Research program (No. 2012SC21), National Natural Science Foundation of China (No. 20976066), Fundamental Research Funds for the Central Universities (No. 2011PY152) and Key Science and Technology Program of Wuhan, China (No. 201120722218).

References

Abe, K., Iwamoto, S., & Yano, H. (2007). Obtaining cellulose nanofibers with a uniform width of 15 nm from wood. *Biomacromolecules*, *8*(10), 3276–3278.
Appaw, C., Gilbert, R. D., & Khan, S. A. (2007). Viscoelastic behavior of cellulose acetate in a mixed solvent system. *Biomacromolecules*, *8*(5), 1541–1547.
ASTM, D 871-96. Standard tests for cellulose acetate.
Beecroft, L. L., & Ober, C. K. (1997). Nanocomposite materials for optical applications. *Chemistry of Materials*, *9*(6), 1302–1317.
Cao, Y., Wu, J., Meng, T., Zhang, J., He, J., Li, H. Q., et al. (2007). Acetone-soluble cellulose acetates prepared by one-step homogeneous acetylation of cornhusk cellulose in an ionic liquid 1-allyl-3-methylimidazolium chloride (AmimCl). *Carbohydrate Polymers*, *69*(4), 665–672.
Cerqueira, D. A., Filho, G. R., & Meireles, C. S. (2007). Optimization of sugarcane bagasse cellulose acetylation. *Carbohydrate Polymers*, *69*(3), 579–582.
Edgar, K. J., Buchanan, C. M., Debenham, J. S., Rundquist, P. A., Seiler, B. D., Shelton, M. C., et al. (2001). Advances in cellulose ester performance and application. *Progress in Polymer Science*, *26*(9), 1605–1688.
He, J. X., Ming, Z., Cui, S. H., & Wang, Y. S. (2009). High-quality cellulose triacetate prepared from bamboo dissolving pulp. *Journal of Applied Polymer Science*, *113*(1), 456–465.
Hurtubise, F. G. (1962). The analytical and structural aspects of the infrared spectroscopy of cellulose acetate. *Tappi*, *45*(6), 460–465.
Li, D., & Xia, Y. N. (2004). Electrospinning of nanofibers: Reinventing the wheel? *Advanced Materials*, *16*(14), 1151–1170.
Liu, Y. P., & Hu, H. (2008). X-ray diffraction study of bamboo fibers treated with NaOH. *Fibers and Polymers*, *9*(6), 735–739.
Liu, D. G., Zhong, T. H., Chang, P. R., Li, K. F., & Wu, Q. L. (2010). Starch composites reinforced by bamboo cellulosic crystals. *Bioresource Technology*, *101*(7), 2529–2536.
Marcotte, M., Hoshahili, A. R. T., & Ramaswamy, H. S. (2001). Rheological properties of selected hydrocolloids as a function of concentration and temperature. *Food Research International*, *34*(8), 695–703.
Nitayaphat, W., Jiratumnukul, N., Charuchinda, S., & Kittinaovarat, S. (2009). Mechanical properties of chitosan/bamboo charcoal composite films made with normal and surface oxidized charcoal. *Carbohydrate Polymers*, *78*(3), 444–448.
Novak, B. M. (1993). Hybrid nanocomposite materials-between inorganic glasses and organic polymers. *Advanced Materials*, *5*(6), 422–433.
Rao, M. A. (2007). *Rheology of fluid and semisolid foods principles and applications* (2nd ed.). New York: Springer.
Rodrigues, F. G., Silva, R. C., Meireles, C. S., Assuncao, R. M. N., & Otaguro, H. (2005). Water flux through blends from waste materials: Cellulose acetate (from sugar cane bagasse) with polystyrene (from plastics cups). *Journal of Applied Polymer Science*, *96*(2), 516–522.
Sassi, J. F., & Chanzy, H. (1995). Ultrastructural aspects of the acetylation of cellulose. *Cellulose*, *2*(2), 111–127.
Sigmund, W., Yuh, J., Park, H., Maneeratana, V., Pyrgiotakis, G., & Daga, A. (2006). Processing and structure relationships in electrospinning of ceramic fiber systems. *Journal of the American Ceramic Society*, *89*(2), 395–407.
Steinmeier, H. (2004). Acetate manufacturing, process and technology. *Macromolecular Symposia*, *208*(1), 49–60.
Thorvaldsson, A., Stenhamre, H., Gatenholm, P., & Walkenström, P. (2008). Electrospinning of highly porous scaffolds for cartilage regeneration. *Biomacromolecules*, *9*(3), 1044–1049.
Wan, Z. L., Xiong, Z. Y., Ren, H. L., Huang, Y. Y., Liu, H. X., Xiong, H. G., et al. (2011). Graft copolymerization of methyl methacrylate onto bamboocellulose under microwave irradiation. *Carbohydrate Polymers*, *83*(1), 264–269.
Xu, X. J., Li, F. X., Yu, J. Y., & Cao, A. M. (2008). Effects of molecular weight and rheological properties on spinnability of biodegradable PBST copolyesters. *International Journal of Nonlinear Sciences and Numerical Simulation*, *9*(1), 31–36.
Yano, H., Sugiyama, J., Nakagaito, A. N., Nogi, M., Matsuura, T., Hikita, M., et al. (2005). Optically transparent composites reinforced with networks of bacterial nanofibers. *Advanced Materials*, *17*(2), 153–155.